Unitary chiral dynamics in $J/\Psi \to VPP$ decays and the role of scalar mesons

L. Roca[1], J. E. Palomar[1], E. Oset[1] and H. C. Chiang[2]

[1] *Departamento de Física Teórica and IFIC, Centro Mixto Universidad de Valencia-CSIC, Institutos de Investigación de Paterna, Aptdo. 22085, 46071 Valencia, Spain*

[2] *Institute of High Energy Physics, Chinese Academy of Sciences, Beijing 100039, China*

February 1, 2008

Abstract

We make a theoretical study of the J/Ψ decays into $\omega\pi\pi$, $\phi\pi\pi$, $\omega K\bar{K}$ and $\phi K\bar{K}$ using the techniques of the chiral unitary approach stressing the important role of the scalar resonances dynamically generated through the final state interaction of the two pseudoscalar mesons. We also discuss the importance of new mechanisms with intermediate exchange of vector and axial-vector mesons and the role played by the OZI rule in the $J/\Psi\phi\pi\pi$ vertex, quantifying its effects. The results nicely reproduce the experimental data for the invariant mass distributions in all the channels considered.

1 Introduction

The J/Ψ decay into a pseudoscalar meson pair and a vector meson has been claimed to be one of the most suited reactions to study the long controversial nature of the scalar mesons, and much work in this direction has been done both theoretically [1–6] and experimentally [7–10]. The nature of the scalar mesons is controversial and the interpretation as $q\bar{q}$ mesons or as meson-meson molecules has mainly centered the discussion [11]. When trying to extract the physical properties of the scalar resonances from experimental data, one has to be extremely careful in fitting the theoretical models to the data since the 'bumps' or 'peaks' in the invariant mass distributions are much influenced by the particular dynamics of the production mechanisms. For instance, the $f_0(980)$ peak in the $\phi \to \pi^0\pi^0\gamma$ decay is distorted with respect to its shape in other reactions, because gauge invariance of the production mechanisms introduces a factor of the photon momentum which vanishes at the highest $\pi\pi$ invariant mass, and grows fast as this mass decreases passing through the $f_0(980)$ peak [12–14]. Other sources of distortion appear due to interferences with other mechanisms or non trivial effects due to the proximity of thresholds [14, 15].

Using the $J/\Psi \to \phi(MM)$ decay, the authors of [2] found the $f_0(980)$ meson to have a pole structure different to a $K\bar{K}$ molecule in contrast to the findings of [5]. In [6] the authors found that only a pole in the second Riemann sheet was necessary to describe the $J/\Psi \to \phi(\pi\pi, K\bar{K})$ data. Concerning the σ meson, the $\pi\pi$ mass distribution of the experimental $J/\Psi \to \omega\pi\pi$ decay clearly shows an enhancement at around 500 MeV, which has been tried to be explained as a genuine σ meson described with Breit-Wigner shapes [1, 7, 8].

In the last years, a chiral unitary coupled channel approach [16–18] has proved to be successful in describing meson-meson interactions in all channels up to energies ~ 1.2 GeV, far beyond the natural limit of applicability of the standard Chiral Perturbation Theory (ChPT), which is $\sim$ 500 MeV where the pole of the lightest resonance, the σ meson, appears. In [16] the inverse amplitude method in coupled channels is used while in [17] the N/D unitary method is exploited and it is shown to be equivalent to a resummation of the loops implemented in a coupled channel Bethe-Salpeter equation using as kernel the lowest order ChPT Lagrangian [19]. In this approach the scalar mesons, which are a matter of concern in the present work, rise up naturally as dynamically generated resonances, in the sense that, without being included as explicit degrees of freedom, they appear as poles in the s-wave meson-meson scattering amplitudes. Concerning the J/Ψ decays of interest in the present work, the chiral unitary approach was used in Ref. [4] for these J/Ψ decays in order to evaluate the scalar form factor. In Ref. [3] a similar technique was used to implement the meson-meson rescattering in the same processes.

On the other hand, as pointed out in Ref. [4], the data on these J/Ψ decays can be used to quantify the violation of the second order Okubo-Zweig-Iizuka (OZI) rule in the 0^{++} sector. In Ref. [4], it was found that a sizeable violation of the OZI rule was necessary to describe the data, in agreement with the arguments of Refs. [20, 21] where the OZI rule violation in the scalar sector is justified.

Given the controversy in the explanation of the nature of the scalar mesons from these J/Ψ decays and the extraction of their 'physical' properties from the experimental data, the aim of the present work is to make a consistent and comprehensive description of the $J/\Psi \to VPP$ decays, including all the mechanisms able to influence the region of pseudoscalar pair invariant masses up to ~ 1.1 GeV, addressing the main problems described above concerning the role played by the scalar mesons and the OZI rule. First of all, in Section 2.1, we will address the same mechanisms used in Ref. [4], essentially the effect of meson rescattering using techniques of the chiral unitary approach, on top of the tree level $J/\Psi \to VPP$ amplitude provided by a phenomenological local Lagrangian. We use $SU(3)$ arguments to relate the different channels and show the equivalence to the formalism of Ref. [4] and its relation to the OZI rule violation. In Sections 2.2 and 2.3 we explain other mechanisms with sequential exchange of vector and axial-vector mesons and, as an important novelty, the meson-meson final state interaction. For the vertices needed in these mechanisms we use previous Lagrangians [22–24] and propose new ones for those involving the J/Ψ meson. In the Results section we make a thorough study of the role played by the scalar mesons and the OZI rule in these decays and compare our results with experimental data for $\omega\pi\pi$, $\phi\pi\pi$, $\omega K\bar{K}$ and $\phi K\bar{K}$ from DM2 [8,9], MARK-III [10] and the recent BES [7]

experiments.

2 The model for $J/\Psi \to VPP$ decay

We proceed to construct our model by addressing different mechanisms which, by analogy to other physical processes previously studied, can significantly contribute to the $J/\Psi \to VPP$ decays up to PP invariant mass of around 1.2 GeV, where the scalar resonances σ and $f_0(980)$ play a very important role. Following the framework of the chiral unitary approach, we will implement the final meson-meson state interaction in order to generate dynamically the scalar resonances involved.

First of all let us define the nomenclature we will use for the kinematics along this work: the decay we are considering is

$$J/\Psi(\epsilon^*, q^*) \to P_1(p_1) + P_2(p_2) + V(\epsilon, q) \tag{1}$$

with ϵ^* and ϵ the polarization vectors of the J/Ψ and the final vector meson respectively. The expression of the differential decay width with respect to the invariant mass of the two pseudoscalars in the J/Ψ rest frame can be evaluated as

$$\frac{d\Gamma}{dM_I} = \frac{M_I}{64\pi^3 M^2} \int_{m_1}^{M-\omega_q-m_2} d\omega_1 \overline{\sum} |t|^2 \Theta(1 - \cos\bar{\theta}^2) \tag{2}$$

where M is the J/Ψ mass, M_I is the invariant mass of the two pseudoscalars, ω_i the on-shell energy of the corresponding particle, Θ the step function and $\cos\bar{\theta} = \frac{(M-\omega_q-\omega_1)^2 - m_2^2 - |\vec{q}|^2 - |\vec{p}_1|^2}{2|\vec{q}||\vec{p}_1|}$, where $\bar{\theta}$ is the angle between $\vec{p}_1$ and $\vec{q}$. The t-matrix can be expressed as

$$t \equiv \epsilon^*_\mu \epsilon_\nu t^{\mu\nu} \tag{3}$$

and therefore the polarization sum is

$$\sum |t|^2 = \sum_{\mu\mu'\nu\nu'} \left(-g_{\mu\mu'} + \frac{q^*_\mu q^*_{\mu'}}{M^2}\right) \left(-g_{\nu\nu'} + \frac{q_\nu q_{\nu'}}{M_V^2}\right) t^{\mu\nu} t^{*\mu'\nu'} \tag{4}$$

In the next subsections we evaluate the different contributions to the amplitude.

2.1 The $J/\Psi PPV$ vertex with meson loops

The first mechanisms to be considered are those involving a direct coupling of the J/Ψ to the two pseudoscalars and the vector, implementing the final state interaction of the pseudoscalars pair, as is depicted in Fig. 1 for the $J/\Psi \to \omega\pi^+\pi^-$ channel.

The thick dot in Fig. 1 means that one is considering the full $\pi\pi(K\bar{K}) \to \pi^+\pi^-$ t-matrix, involving the loop resummation of the Bethe-Salpeter equation of Ref. [19] and no just the lowest order $\pi\pi(K\bar{K}) \to \pi^+\pi^-$ amplitude. Actually this loop resummation is what dynamically generates the scalar resonances, in the sense that the scalars are not

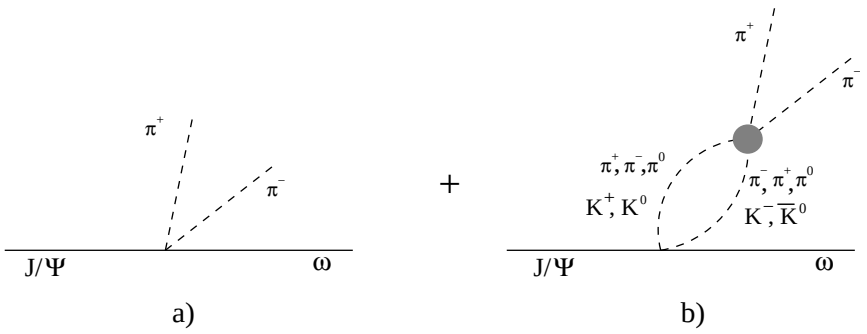

Figure 1: Diagrams with direct $J/\Psi VPP$ vertex at tree level, a), and with the iterated meson loops, b).

explicitly included in the model but they appear naturally as poles in the meson-meson scattering amplitude [19].

For the evaluation of these diagrams we need to know the vertex accounting for the transition of the J/Ψ into a vector meson and a pseudoscalar meson pair. We will consider the pseudoscalar pair having the vacuum quantum numbers, $J^{PC} = 0^{++}$, since, as mentioned in the introduction, the J/Ψ decays considered in the present work are dominated by the scalar sector at the energies that we are interested in. Similarly to what is done in Ref. [4] we write a contact term of the form

$$\Psi_\mu V^\mu \phi\phi'; \tag{5}$$

where Ψ_μ, V^μ and $\phi\phi'$ are the fields of J/Ψ, vector and pseudoscalar mesons respectively, which according to Ref. [4] is accurate enough since any other possible structures containing derivatives of the fields provide small momentum dependences, given the large J/Ψ mass.

The relative weights between the different channels can be obtained using $SU(3)$ arguments in the following way: the physical meson-meson states can be decomposed in terms of the basis states of the singlet ($\bar{S}_1$), symmetric-octet ($\bar{S}_8^s$) and antisymmetric-octet ($\bar{S}_8^a$) representations of $SU(3)$ by means of the $SU(3)$ Clebsch-Gordan coefficients. This decomposition gives:

$$\begin{aligned} |K\bar{K}> &= -\frac{1}{2\sqrt{2}}|\bar{S}_1> -\frac{1}{2\sqrt{5}}|\bar{S}_8^s> -\frac{1}{2}|\bar{S}_8^a> \\ |\pi\pi> &= -\frac{1}{2\sqrt{2}}|\bar{S}_1> +\frac{1}{\sqrt{5}}|\bar{S}_8^s>, \end{aligned} \tag{6}$$

where we have also used a minus sign in the phase of the π^+ and K^- states.

From Eq. (6), and with the Wigner-Eckart theorem in mind and taking into account that the J/Ψ can be considered as a $SU(3)$ singlet, it is direct to write the following matrix elements:

$$
\begin{aligned}
< V_1|t|K\bar{K} > &= -\frac{1}{2\sqrt{2}} < V_1|t|\bar{S}_1 > \equiv -\frac{1}{2\sqrt{2}} t_1 \\
< V_8^s|t|K\bar{K} > &= -\frac{1}{2\sqrt{5}} < V_8^s|t|\bar{S}_8^s > \equiv -\frac{1}{2\sqrt{5}} t_8^s \\
< V_1|t|\pi\pi > &= -\frac{1}{2\sqrt{2}} < V_1|t|\bar{S}_1 > \equiv -\frac{1}{2\sqrt{2}} t_1 \\
< V_8^s|t|\pi\pi > &= -\frac{1}{\sqrt{5}} < V_8^s|t|\bar{S}_8^s > \equiv \frac{1}{\sqrt{5}} t_8^s,
\end{aligned} \tag{7}
$$

where t_1 and t_8^s are the reduced matrix elements which we will consider as unknown coefficients. Actually, t_1 and t_8^s will be the only two free parameters in all the model described along the present work. Given the symmetry $K\bar{K} \leftrightarrow \bar{K}K$ in s-wave and that $\bar{K}K$ has a coefficient $+1/2$ for the $|\bar{S}_8^a >$ state, instead of $-1/2$ in Eq. (6) for $K\bar{K}$, the matrix elements with the antisymmetric octet state vanish.

On the other hand, considering ideal mixing between the V_8 and V_1 states (we omit the index "s" for symmetric in what follows), we can write the following decomposition in terms of the physical ϕ and ω meson states:

$$
V_1 = \sqrt{\frac{2}{3}}\omega + \frac{1}{\sqrt{3}}\phi, \qquad V_8 = \frac{1}{\sqrt{3}}\omega - \sqrt{\frac{2}{3}}\phi. \tag{8}
$$

Using Eqs. (7) and (8) and including also the polarization vectors of the J/Ψ, ϵ^*, and the vector meson, ϵ, the amplitudes for the different contact terms involving the J/Ψ, one vector and two pseudoscalars needed to evaluate the diagrams of Fig. 1, are:

$$
\begin{aligned}
t_{J/\Psi\phi K\bar{K}} &= -\frac{1}{\sqrt{6}}\left(\frac{1}{2}t_1 - \frac{1}{\sqrt{5}}t_8\right)\,\epsilon^*\cdot\epsilon \\
t_{J/\Psi\omega K\bar{K}} &= -\frac{1}{2\sqrt{3}}\left(t_1 + \frac{1}{\sqrt{5}}t_8\right)\,\epsilon^*\cdot\epsilon \\
t_{J/\Psi\phi\pi\pi} &= -\frac{1}{\sqrt{6}}\left(\frac{1}{2}t_1 + \frac{2}{\sqrt{5}}t_8\right)\,\epsilon^*\cdot\epsilon \\
t_{J/\Psi\omega\pi\pi} &= -\frac{1}{2\sqrt{3}}\left(t_1 - \frac{2}{\sqrt{5}}t_8\right)\,\epsilon^*\cdot\epsilon.
\end{aligned} \tag{9}
$$

At this point it is worth mentioning the implications of the OZI rule in this decays. A thorough study and explanation of the role played by the OZI rule in the J/Ψ decays into a ϕ meson and two pseudoscalars was done in Ref. [4]. For the purpose of the present work it is enough to point out that, due to the non-existence of direct quark line connexion between the strange and up or down quarks, the $J/\Psi \to \phi\pi\pi$ decay is suppressed to next order in α_s with respect to the other channels. Should the OZI rule be exact, $t_{J/\Psi\phi\pi\pi}$ would be zero, implying that $t_1 = (-4/\sqrt{5})t_8$. Sizeable deviations from this numerical

relation would point out to a necessary deviation from the OZI rule. This is something to be expected since this rule is only well founded for the large N_c limit of QCD and the 0^{++} sector is not well described in this limit. In Ref. [4] a different approach was followed parametrizing the Lagrangian in terms of a scalar source S which plays the role of the pseudoscalar pairs with scalar quantum numbers in our model, and this scalar is written in terms of quark fields as

$$\bar{\Psi}_\mu V^\mu S \tag{10}$$

and

$$S \equiv \bar{s}s + \lambda_\phi \frac{1}{\sqrt{2}}(\bar{u}u + \bar{d}d). \tag{11}$$

In this way, the λ_ϕ parameter accounts for the relative weight of the non-strange quark content of the scalar sources. Therefore it quantifies the OZI rule violation in the case of two pions in the scalar channel connected to the ϕ and the J/Ψ. In Ref. [4] the following relations of the quark-antiquark operators in terms of the meson-meson fields were obtained from the mass term of the lowest order ChPT Lagrangian, (see that reference for details):

$$\begin{aligned}
\bar{u}u &= -f^2 B_0 \left[1 - \frac{1}{f^2}\left(\pi^+\pi^- + K^+K^- + \frac{(\pi^0)^2}{2} + \frac{\eta_8^2}{6} + \frac{\pi^0\eta_8}{\sqrt{3}}\right) + ...\right] \\
\bar{d}d &= -f^2 B_0 \left[1 - \frac{1}{f^2}\left(\pi^+\pi^- + K^0\overline{K}^0 + \frac{(\pi^0)^2}{2} + \frac{\eta_8^2}{6} - \frac{\pi^0\eta_8}{\sqrt{3}}\right) + ...\right] \\
\bar{s}s &= -f^2 B_0 \left[1 - \frac{1}{f^2}\left(K^+K^- + K^0\overline{K}^0 + \frac{2}{3}\eta_8^2\right) + ...\right]
\end{aligned} \tag{12}$$

where the dotted points represent higher order in the meson fields. The small non-strange content of the pions is clearly manifest in the last of these equations since the pion fields would appear at higher orders in the meson fields. Introducing the octet and singlet scalar sources, V_8 and V_1 respectively, the Lagrangian for the contact term interaction can be expressed as

$$\hat{g}\,\Psi_\mu(V_8^\mu S_8 + \nu V_1^\mu S_1) \tag{13}$$

with ν an unknown parameter accounting for the relative weight between the singlet and octet couplings, which in Ref. [4] is related to the λ_ϕ parameter of Eq. (11).
One can introduce the scalar sources S_ω and S_ϕ in an analogous way to Eq. (8):

$$S_1 = \sqrt{\frac{2}{3}}S_\omega + \frac{1}{\sqrt{3}}S_\phi, \qquad S_8 = \frac{1}{\sqrt{3}}S_\omega - \sqrt{\frac{2}{3}}S_\phi, \tag{14}$$

where in a quark model language, consistently with the transformation properties under SU(3), we can write:

$$S_\phi = \bar{s}s \quad \text{and} \quad S_\omega = \frac{1}{\sqrt{2}}(\bar{u}u + \bar{d}d)\ . \tag{15}$$

Combining Eqs. (12), (13), (14) and (15) one obtains the following amplitudes for the different contact terms involving the J/Ψ, one vector and two pseudoscalars:

$$\begin{aligned}
t_{J/\Psi\phi K\bar{K}} &= -\frac{\tilde{g}}{3}(2\nu+1)\,\epsilon^*\cdot\epsilon \\
t_{J/\Psi\omega K\bar{K}} &= -\frac{\tilde{g}}{3\sqrt{2}}(4\nu-1)\,\epsilon^*\cdot\epsilon \\
t_{J/\Psi\phi\pi\pi} &= -\frac{2\tilde{g}}{3}(\nu-1)\,\epsilon^*\cdot\epsilon \\
t_{J/\Psi\omega\pi\pi} &= -\frac{\sqrt{2}\tilde{g}}{3}(2\nu+1)\,\epsilon^*\cdot\epsilon.
\end{aligned} \tag{16}$$

with $\nu = \frac{\sqrt{2}+2\lambda_\phi}{\sqrt{2}-\lambda_\phi}$ and $\tilde{g} \equiv \hat{g}B_0$ where B_0 is the constant appearing in the mass term of the chiral Lagrangian [25]. In these amplitudes $\tilde{g}$ and ν (or equivalently the OZI violation parameter λ_ϕ) are the two free parameters. Note that the exact accomplishment of the OZI rule would require $\lambda_\phi = 0$ (see Eq. (11)), and consequently $\nu = 1$, and therefore it would imply the third equation of Eqs. (16) to be zero.

Comparing Eqs. (9) and (16) it is immediate to see the equivalence between the two different treatments of the $SU(3)$ symmetry by writing

$$t_1 = 4\sqrt{\frac{2}{3}}\tilde{g}\nu \qquad , \qquad t_8 = -\sqrt{\frac{10}{3}}\tilde{g}. \tag{17}$$

The treatment of Eqs. (5) to (9) is very intuitive and easy while the one from Eqs. (11) to (17) has the virtue of expressing the amplitudes directly in terms of the OZI rule violating parameter. In order to favour comparison of our results with those of Ref. [4], we shall adopt their nomenclature, using $\tilde{g}$ and λ_ϕ as free parameters instead of t_1 and t_8.

All this said, we can already write the amplitudes for the diagrams depicted in Fig. 1 for all the channels of concern in the present work:

$$\begin{aligned}
t_{J/\Psi\to\omega\pi^+\pi^-} &= -\tilde{g}\epsilon^*\epsilon\frac{\sqrt{2}}{3}\left[\frac{4\nu-1}{\sqrt{3}}G_{KK}t^{I=0}_{KK,\pi\pi} + (1+2\nu)\left(1+G_{\pi\pi}t^{I=0}_{\pi\pi,\pi\pi}\right)\right] \\
t_{J/\Psi\to\phi\pi^+\pi^-} &= -\tilde{g}\epsilon^*\epsilon\frac{2}{3}\left[\frac{1+2\nu}{\sqrt{3}}G_{KK}t^{I=0}_{KK,\pi\pi} + (\nu-1)\left(1+G_{\pi\pi}t^{I=0}_{\pi\pi,\pi\pi}\right)\right] \\
t_{J/\Psi\to\omega K^+K^-} &= -\tilde{g}\epsilon^*\epsilon\frac{1}{3\sqrt{2}}\left[(4\nu-1)(1+G_{KK}t^{I=0}_{KK,KK}) + \sqrt{3}(1+2\nu)G_{\pi\pi}t^{I=0}_{\pi\pi,KK}\right] \\
t_{J/\Psi\to\phi K^+K^-} &= -\tilde{g}\epsilon^*\epsilon\frac{1}{3}\left[(1+2\nu)(1+G_{KK}t^{I=0}_{KK,KK}) + \sqrt{3}(\nu-1)G_{\pi\pi}t^{I=0}_{\pi\pi,KK}\right]
\end{aligned} \tag{18}$$

In Eq. (18) $G_{\pi\pi}$ and G_{KK} are the ordinary two meson loop functions regularized by means of a cutoff of the order of 1 GeV, $t^{I=0}_{MM,M'M'}$ are the isospin zero $MM \to M'M'$ transition amplitudes, accounting for the resummation of the iterated loops, evaluated

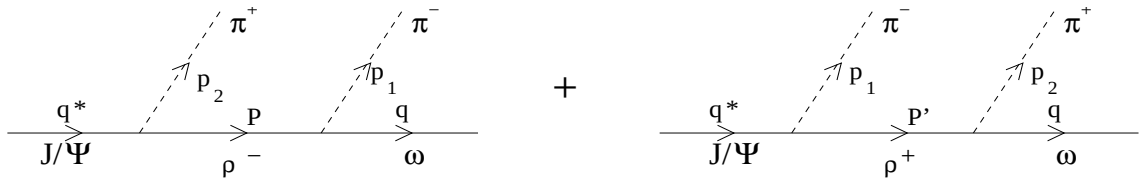

Figure 2: Diagrams for the tree level mechanisms with sequential vector meson exchange.

with the techniques of the chiral unitary approach of Ref. [19]. Note that the meson-meson scattering amplitudes have been factorized on shell out of the loops as was justified in Ref. [19]. In Eq. (18) we have also taken into account that

$$\begin{aligned} < \pi^+\pi^- + \pi^-\pi^+ + \pi^0\pi^0|t_m|\pi^+\pi^- > &= 2t^{I=0}_{\pi\pi,\pi\pi} \\ < K^+K^- + K^0\bar{K}^0|t_m|\pi^+\pi^- > &= \frac{2}{\sqrt{3}}t^{I=0}_{KK,\pi\pi} \\ < K^+K^- + K^0\bar{K}^0|t_m|K^+K^- > &= t^{I=0}_{KK,KK} \\ < \pi^+\pi^- + \pi^-\pi^+ + \pi^0\pi^0|t_m|K^+K^- > &= \sqrt{3}t^{I=0}_{KK,\pi\pi} \end{aligned} \tag{19}$$

where the unitary normalization for the states of Ref. [19] has been used.

2.2 Sequential vector and axial-vector meson exchange mechanisms: tree level

Previous works on ρ, ω [22, 26] and ϕ [14, 27, 28] decays into two pseudoscalars and one photon, showed that the mechanisms where the initial vector meson decays into a pseudoscalar and another vector meson, and this latter one decays itself into a pseudoscalar and one photon, play an important role. The strong analogy with the decays studied in the present work suggests to study the role played in these J/Ψ decays by these kind of mechanisms, not previously considered in other works. On the other hand, the strong meson-meson scattering of the final pseudoscalar mesons, specially in the scalar channel, which we will discuss in subsection 2.3, makes definitively necessary their study.

In what follows we will explicitly discuss the $J/\Psi \to \omega\pi^+\pi^-$ channel, referring to the Appendix for the formulae of the other channels since they are analogous.

In Fig. 2 the two allowed diagrams at tree level for the sequential vector meson exchange are depicted, including the notation for the momenta.

For the evaluation of the vector-vector-pseudoscalar (VVP) vertex we use the same Lagrangians as in [22, 23]

$$\mathcal{L}_{VVP} = \frac{G}{\sqrt{2}}\epsilon^{\mu\nu\alpha\beta}\langle \partial_\mu V_\nu \partial_\alpha V_\beta P\rangle \tag{20}$$

where $\langle\rangle$ means $SU(3)$ trace, $G = 0.016$ MeV^{-1} and V (P) are the usual vector (pseudoscalar) $SU(3)$ matrices. In an analogous way, we can use the following Lagrangian for

the $J/\Psi VP$ vertex:

$$\mathcal{L}_{\Psi VP} = \frac{\overline{G}}{\sqrt{2}}\epsilon^{\mu\nu\alpha\beta}\langle\partial_\mu\Psi_\nu\partial_\alpha V_\beta P\rangle = \frac{\overline{G}}{\sqrt{2}}\epsilon^{\mu\nu\alpha\beta}\partial_\mu\Psi_\nu\langle\partial_\alpha V_\beta P\rangle. \tag{21}$$

where in the last step the J/Ψ field, $SU(3)$ singlet, is factorized out of the $SU(3)$ trace. From the experimental $J/\Psi \to VP$ decay widths from the PDG [29], we obtain the numerical value of the coupling constant with its error: $\overline{G} = (1.44 \pm 0.05) \times 10^{-6}$ MeV^{-1}, with the overall sign unknown. The uncertainties coming from the sign and the experimental errors will be discussed in the Results section.

With the Lagrangians of Eqs. (20) and (21), the amplitude for the diagrams depicted in Fig. 2 reads

$$t = -\frac{G\overline{G}}{\sqrt{2}}\left[\frac{P^2\{a\} + \{b(P)\}}{M_\rho^2 - P^2 - iM_\rho\Gamma_\rho(P^2)} + \frac{P'^2\{a\} + \{b(P')\}}{M_\rho^2 - P'^2 - iM_\rho\Gamma_\rho(P'^2)}\right] \tag{22}$$

where $P = p_1 + q$, $P' = p_2 + q$ and

$$\begin{aligned}\{a\} &= \epsilon^*\cdot\epsilon\ q^*\cdot q - \epsilon^*\cdot q\ \epsilon\cdot q^* \\ \{b(P)\} &= -\epsilon^*\cdot\epsilon\ q^*\cdot P\ q\cdot P - \epsilon\cdot P\ \epsilon^*\cdot P\ q^*\cdot q + \epsilon^*\cdot q\ \epsilon\cdot P\ q^*\cdot P + \epsilon\cdot q^*\ \epsilon^*\cdot P\ q\cdot P\end{aligned}$$

In Ref. [14] the important role of the analogous mechanisms considering the exchange of an axial-vector meson with $J^{PC} = 1^{+-}$ or 1^{++} was shown. In Table 1 we show the particles of these octets. In addition one has to consider the mixture of the K_{1B} and K_{1A}

J^{PC}	$I=1$	$I=0$	$I=1/2$
1^{+-}	$b_1(1235)$	$h_1(1170)$, $h_1(1380)$	K_{1B}
1^{++}	$a_1(1260)$	$f_1(1285)$, $f_1(1420)$	K_{1A}

Table 1: Octets of axial-vector mesons.

states to give the physical $K_1(1270)$ and $K_1(1400)$ states:

$$\begin{aligned}K_1(1270) &= \cos(\alpha)K_{1B} - i\sin(\alpha)K_{1A} \\ K_1(1400) &= \sin(\alpha)K_{1B} + i\cos(\alpha)K_{1A}\end{aligned} \tag{23}$$

with $\alpha \simeq 45$ degrees[1].

In the $J/\Psi \to \omega\pi^+\pi^-$ decay, the mechanisms are equivalent to those of Fig. 2 substituting the intermediate ρ meson by the $b_1(1235)$. The non negligible contribution of these new mechanisms was already pointed out in Ref. [3]. For the evaluation of these diagrams we need the couplings of the axial-vectors to one vector and one pseudoscalar and the J/Ψ

[1]It is worth mentioning that in [24, 30] two more possible solutions for the mixing angle between the I=1/2 members of the axial-vector octets were found around 30 and 60 degrees . This uncertainty will be taken into account in the evaluation of the theoretical error band of the final results.

to one axial vector and one pseudoscalar. For the first one we use the phenomenological Lagrangian proposed in Ref. [24] which successfully describes the experimental branching ratios of one axial-vector decay into one vector plus one pseudoscalar and was used in [14] in radiative ϕ decay. This Lagrangian is:

$$\mathcal{L}_{A(B)VP} = D\langle V_{\mu\nu}\{B^{\mu\nu}, P\}\rangle - iF\langle V_{\mu\nu}[A^{\mu\nu}, P]\rangle \tag{24}$$

with $D = -1000 \pm 120$ MeV; $F = 1550 \pm 150$ MeV and B and A are the $SU(3)$ matrices, in the tensor formalism of [31], containing the octet of 1^{+-} and 1^{++} respectively. In this tensor formalism the fields $W_{\mu\nu} \equiv V_{\mu\nu}$, $B_{\mu\nu}$, $A_{\mu\nu}$ are normalized such that

$$< 0|W_{\mu\nu}|W; P, \epsilon >= \frac{i}{M_W}\left[P_\mu\, \epsilon_\nu(W) - P_\nu\, \epsilon_\mu(W)\right] \tag{25}$$

In addition the propagators with the tensor fields are given by [31]

$$\begin{aligned} &< 0|T\{W_{\mu\nu}W_{\rho\sigma}\}|0 >= i\mathcal{D}_{\mu\nu\rho\sigma} = \\ &= i\frac{M_W^{-2}}{M_W^2 - P^2 - i\epsilon}\left[g_{\mu\rho}\, g_{\nu\sigma}\,(M_W^2 - P^2) + g_{\mu\rho}\, P_\nu\, P_\sigma - g_{\mu\sigma}\, P_\nu\, P_\rho - (\mu \leftrightarrow \nu)\right]. \end{aligned} \tag{26}$$

For the vertex involving the J/Ψ, one axial and one pseudoscalar meson we can replace in Eq. (24) $V_{\mu\nu}$ by the J/Ψ field, $\Psi_{\mu\nu}$, where, since $\Psi_{\mu\nu}$ can be considered as an $SU(3)$ singlet, it factorizes out of the $SU(3)$ trace. Therefore we have

$$\begin{aligned} \mathcal{L}_{A(B)\Psi P} &= \frac{\overline{D}}{2}\Psi_{\mu\nu}\langle\{B^{\mu\nu}, P\}\rangle - i\overline{F}\Psi_{\mu\nu}\langle[A^{\mu\nu}, P]\rangle \\ &= \overline{D}\Psi_{\mu\nu}\langle B^{\mu\nu}P\rangle \end{aligned} \tag{27}$$

since $\langle[A^{\mu\nu}, P]\rangle = 0$. In Eq. (27) we have obtained that there is no direct coupling of the J/Ψ to the octet of 1^{++} axial-vector mesons and one pseudoscalar, something that is in agreement with the absence of experimental evidence of these decays [29]. This makes us confident in the phenomenological reliability of the Lagrangian of Eq. (27). From the PDG experimental values of the J/Ψ decay into an axial-vector meson and a pseudoscalar we obtain $\overline{D} = 2.12 \pm 0.24$ MeV, with an overall undetermined sign which will be discussed in the Results section.

With the Lagrangians of Eqs. (24) and (27), the amplitude for the tree level sequential mechanism with the exchange of an axial-vector meson is

$$\begin{aligned} t = \frac{4\sqrt{2}D\overline{D}}{Mm_\omega M_b^2}\Bigg[&(\epsilon^*\cdot\epsilon\; q^*\cdot q - \epsilon^*\cdot q\;\epsilon\cdot q^*)\;+\;\frac{1}{M_b^2 - P^2 - iM_b\Gamma_b(P^2)}\cdot \\ &\cdot\;(\epsilon^*\cdot\epsilon\; q^*\cdot P\; q\cdot P + \epsilon\cdot P\;\epsilon^*\cdot P\; q^*\cdot q - \epsilon^*\cdot q\;\epsilon\cdot P\; q^*\cdot P - \epsilon\cdot q^*\;\epsilon^*\cdot P\; q\cdot P)\Bigg] \end{aligned} \tag{28}$$

plus the crossed term, with P' instead of P.

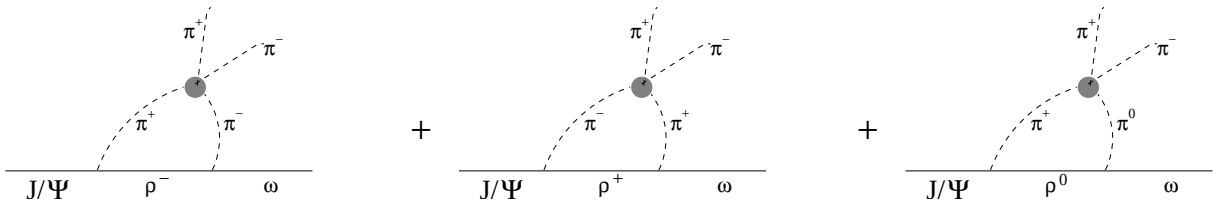

Figure 3: Sequential vector meson exchange diagrams with final state interaction of pions

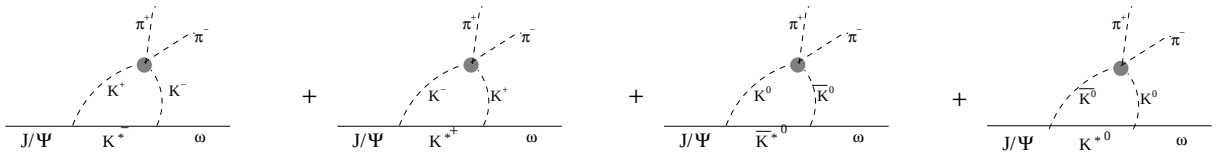

Figure 4: Sequential vector meson exchange diagrams with final state interaction of kaons

2.3 Final state interaction in the sequential vector and axial-vector exchange mechanisms

Since the meson-meson interaction is strong in the region of invariant masses relevant in the present reaction, specially in the scalar channel, we next consider the final state interaction of the two pions in the sequential vector meson mechanism (see Fig. 3) but also with kaons in the intermediate states (Fig. 4). Again the thick dot in Figs. 3 and 4 means that one is considering the full meson-meson to $\pi\pi$ t-matrix, involving the loop resummation of the BS equation of Ref. [19] and not just the lowest order amplitude.

To evaluate these diagrams we need to calculate the loop functions containing a vector and two pseudoscalar meson propagators. The evaluation of these three meson loop functions was done in Ref. [14]. We summarize here the main steps:

given the structure of the terms in Eq. (22) we must evaluate the loop integrals

$$i\int \frac{d^4P}{(2\pi)^4}\, P^\mu P^\nu \frac{1}{P^2 - M_b^2 + i\epsilon}\, \frac{1}{(q^* - P)^2 - m_1^2 + i\epsilon}\, \frac{1}{(q - P)^2 - m_2^2 + i\epsilon} \tag{29}$$

where m_1 and m_2 are the masses of the pseudoscalar mesons of the loops and P is the momentum of the vector meson in the loop.

For simplicity we evaluate these integrals in the reference frame where the two meson system has zero momentum. In this frame the J/Ψ and ω trimomentum are the same, $\vec{q}$. At the end we will boost back the $t^{\mu\nu}$-matrix to the J/Ψ rest frame where the phase-space integration and the polarization vectors sum is done.

Given the momentum structure of Eqs. (28) and (22), we need the following integrals, which for dimensional reasons we write as

$$i\int \frac{d^4P}{(2\pi)^4} P^0 P^0 D_1 D_2 D_3 = I_0$$

$$i\int \frac{d^4P}{(2\pi)^4} P^0 P^i D_1 D_2 D_3 = \frac{q^i}{|\vec{q}|} I_1$$
$$i\int \frac{d^4P}{(2\pi)^4} P^i P^j D_1 D_2 D_3 = \delta_{ij} I_a + \frac{q^i q^j}{\vec{q}^{\,2}} I_b \tag{30}$$

where D_1, D_2, D_3 are the three meson propagators of Eq. (29) and the momenta are in the dimeson rest frame. Analytical expressions for the P^0 integration in Eq. (30) can be found in the Appendix of Ref. [14]. The $d^3\vec{P}$ integral is evaluated numerically by means of the same cut off, of the order of 1 GeV, which has been used to regularize the two meson loop in the meson-meson interaction.

With the structure of Eq. (22) and the substitutions of Eq. (30), one can already evaluate the amplitude $t^{\mu\nu}$ for the diagrams of Fig. 3 which, after the proper boost transformation to the J/Ψ rest frame and after some calculations, reads as

$$t^{\mu\nu} = \frac{G\overline{G}}{\sqrt{2}}\, \bar{t}'^{\mu\nu}\, 2t^{I=0}_{\pi\pi,\pi\pi} \tag{31}$$

with

$$\bar{t}'^{\mu\nu} = \begin{pmatrix} 0 & 0 & 0 & 0 \\ \frac{2I_a}{M^2}|\vec{q}|(q^{*0^2}-\vec{q}^{\,2})(q^{*0}-q^0) & \frac{2I_a}{M^2}(q^{*0^2}-\vec{q}^{\,2})(q^{*0}q^0-\vec{q}^{\,2}) & 0 & 0 \\ 0 & 0 & \bar{t}'_{22} & 0 \\ 0 & 0 & 0 & \bar{t}'_{33} \end{pmatrix} \tag{32}$$

where $\bar{t}'_{22} = \bar{t}'_{33} \equiv \vec{q}^{\,2} I_0 - |\vec{q}|(q^0+q^{*0})I_1 - (\vec{q}^{\,2} - 2q^0q^{*0})I_a + q^0q^{*0}I_b$. The matrix $\bar{t}'^{\mu\nu}$ is the proper Lorentz tensor in the J/Ψ rest frame, although for convenience (since the functions I_i are evaluated in the dimeson rest frame) we write the $\bar{t}'^{\mu\nu}$ components in terms of the dimeson rest frame momenta given by

$$q^0 = -\frac{M_I^2 - M^2 + m_\omega^2}{2M_I}, \quad q^{*0} = M_I + q^0 = \frac{M_I^2 + M^2 - m_\omega^2}{2M_I}, |\vec{q}| = |\vec{q^*}| = \sqrt{q^{*0^2} - M^2}. \tag{33}$$

For the kaon loops with exchange of a K^* vector meson, Fig.4, the corresponding expression for the t-matrix, is

$$t^{\mu\nu} = \frac{G\overline{G}}{2\sqrt{2}}\, \bar{t}'^{\mu\nu}\, \frac{4}{\sqrt{3}} t^{I=0}_{KK,\pi\pi}. \tag{34}$$

where we must bear in mind that $\bar{t}'^{\mu\nu}$ has the same structure as in Eq. (32) but the masses and widths of the particles are correspondingly changed.

In an analogous way, we can evaluate the same kind of diagrams but with an intermediate axial-vector meson instead of a vector meson both for pion and kaon intermediate loops. The diagrams are thus the same as Fig. 3 but substituting ρ by b_1 and the same as Fig. 4 substituting K^* by $K_1(1270)$ and $K_1(1400)$. Given the different momentum structure of Eq. (28) with respect to Eq. (22), the t-matrix is slightly different, giving

$$t^{\mu\nu} = \frac{4\sqrt{2}D\overline{D}}{Mm_\omega m_b^2}\left[(q^*\cdot q g^{\mu\nu} - q^\mu q^{*\nu})G_{\pi\pi} - \tilde{t}'^{\mu\nu}\right] 2t^{I=0}_{\pi\pi,\pi\pi}. \quad (35)$$

Given the Lorentz covariance of the factor $(q^*\cdot q g^{\mu\nu} - q^\mu\cdot q^{*\nu})$, coming from the $(\epsilon^*\cdot\epsilon\; q^*\cdot q - \epsilon^*\cdot q\;\epsilon\cdot q^*)$ term in Eq. (28), it can be already evaluated with the momentum variables of the J/Ψ rest frame, that is, $q^* = (M,0,0,0)$, $q^0 = \frac{M^2+m_\omega^2-M_I^2}{2M}$, $|\vec{q}| = \sqrt{q^{0\,2} - m_\omega^2}$. For the $\tilde{t}'^{\mu\nu}$ part, which comes from the part of Eq. (28) that contains a propagator, we still resort to evaluate it in the dimeson rest frame and boost it to the J/Ψ rest frame. Hence, by analogy to Eq. (32), we have

$$\tilde{t}'^{\mu\nu} = \begin{pmatrix} 0 & 0 & 0 & 0 \\ \frac{I_a+I_b-I_0}{M^2}|\vec{q}|(q^{*0\,2}-\vec{q}^{\,2})(q^{*0}-q^0) & \frac{I_a+I_b-I_0}{M^2}(q^{*0\,2}-\vec{q}^{\,2})(q^{*0}q^0-\vec{q}^{\,2}) & 0 & 0 \\ 0 & 0 & \tilde{t}'_{22} & 0 \\ 0 & 0 & 0 & \tilde{t}'_{33} \end{pmatrix} \quad (36)$$

with $\tilde{t}'_{22} = \tilde{t}'_{33} \equiv -q^0 q^{*0} I_0 + |\vec{q}|(q^0+q^{*0})I_1 + (q^{*0}q^0 - 2\vec{q}^{\,2})I_a - \vec{q}^{\,2} I_b$, where in this case the momenta appearing in the expression are those of the dimeson rest frame, Eq. (33). As mentioned before, the I_i integrals have to be evaluated with the appropriate masses and widths of the corresponding mesons in the loops.

For the diagrams with kaon loops and $K_1(1270)$ intermediate exchange, the expression for the t-matrix, obtained in an analogous way, is

$$t^{\mu\nu} = \frac{4}{Mm_\omega m^2_{K_1(1270)}} c\overline{D}\frac{1}{\sqrt{2}}(cD - sF)\left[(q^*\cdot q g^{\mu\nu} - q^\mu q^{*\nu})G_{KK} - \tilde{t}'^{\mu\nu}\right]\frac{4}{\sqrt{3}} t^{I=0}_{KK,\pi\pi}. \quad (37)$$

In Eq. (37), $c \equiv cos(\alpha)$ and $s \equiv cos(\alpha)$ are the cosinus and sinus of the mixing angle, α, between the isospin 1/2 members of the axial-vector octets to give the physical $K_1(1270)$ and $K_1(1400)$ states, Eq. (23). For the diagrams with $K_1(1400)$ intermediate state the amplitude is the same but changing $m_{K_1(1270)} \to m_{K_1(1400)}$, $F \to -F$, $c \to s$ and $s \to c$ and replacing the masses and widths of the $K_1(1270)$ by those of the $K_1(1400)$ in the evaluation of $\tilde{t}'^{\mu\nu}$.

The expressions for the amplitudes of all the mechanisms corresponding to the other channels, $(J/\Psi \to \omega K\bar{K}$, $\phi\pi^+\pi^-$, $\phi K\bar{K})$, are given in the Appendix.

3 Results

In the model described so far, the only unknown parameters are the overall strength, $\tilde{g}$, of the mechanisms of Fig. 1 containing the direct $J/\Psi PPV$ vertex, (which we will call in what follows "direct" terms), and the OZI rule violation parameter, λ_ϕ, (see Eq. (18)). The other constants and couplings appearing in the model are theoretically fixed or obtained from direct decays with the PDG values, and their experimental uncertainties will be taken into account when evaluating the theoretical error bands of our results. Therefore, there

is no freedom in the mechanisms different to "direct" terms in the sense that its strength and shape is fixed, up to some sign which will be discussed below. Taken this into account, the philosophy is to fit the full model to invariant mass distributions of the $J/\Psi \to \omega\pi^+\pi^-$ and $J/\Psi \to \phi\pi^+\pi^-$ decay channels to obtain the two free parameters.

The experimental data for $J/\Psi \to \omega\pi^+\pi^-$ is taken from BES [7] and DM2 [8] experiments. For $J/\Psi \to \phi\pi^+\pi^-$ the data has been taken from DM2 [9] and MARK-III [10] experiments. In most experiments the mass distributions are given in arbitrary units. However, it is possible to find the absolute normalization from information given in the papers or by using the branching ratios for each channels from the PDG, given the fact that the experiments provide the data in the full range of invariant mass allowed. This we have done in the present work and is a novelty with respect to former works on the issue. The fact that all mechanisms in our approach, except the "direct" mechanisms, have a fixed strength forces us to carry a fit to absolute data to make meaningful the extracted values of the parameters of the "direct" mechanisms.

Apart from the freedom due to the $\widetilde{g}$ and λ_ϕ parameters, we have the uncertainty in the signs of the $J/\Psi VP$ and $J/\Psi AP$ couplings, $\overline{G}$ and $\overline{D}$ respectively. This uncertainty reflects in our model in only the relative sign between $\overline{G}$ and $\overline{D}$. This is the case in the decays we are studying in the present work since the relative sign with $\widetilde{g}$ is absorbed in the $\widetilde{g}$ itself, which is a free parameter. Therefore, given also the uncertainty in the overall sign of the full amplitude, we will consider $\overline{D}$ to be positive and will explicitly discuss the cases with $\overline{G} > 0$ and $\overline{G} < 0$.

We will consider invariant dimeson masses up to ~ 1200 MeV since this is approximately the maximum range of applicability of the chiral unitary approach techniques used in the evaluation of the meson-meson final state interaction throughout this work. In the $J/\Psi \to \omega\pi^+\pi^-$ channel the tail of the $f_2(1270)$ meson influences the region of high invariant masses and then is the only source of background which is not generated by our theoretical model. Therefore we have phenomenologically included this resonance by fitting an $f_2(1270)$ Breit-Wigner, convoluted by the $J/\Psi \to \omega\pi^+\pi^-$ phase space, to the $f_2(1270)$ peak (not shown in the figures) of the BES and DM2 data, and then we have added it to $d\Gamma/dM_I$. This incoherent sum is accurate enough since the $f_2(1270)$ meson is a D-wave and does not interfere with the scalar $f_0(980)$ which dominates the process at these energies.

We have obtained the two following results for the fits to the $J/\Psi \to \omega\pi^+\pi^-$ and $J/\Psi \to \phi\pi^+\pi^-$ data:

$$\begin{aligned}
&\text{for } \overline{G} > 0 \ : \quad \widetilde{g} = 0.032 \pm 0.001 \quad ; \lambda_\phi = 0.12 \pm 0.03 \quad ; (\frac{\chi^2}{d.o.f.} \simeq 3.4) \\
&\text{for } \overline{G} < 0 \ : \quad \widetilde{g} = 0.015 \pm 0.001 \quad ; \lambda_\phi = 0.20 \pm 0.03 \quad ; (\frac{\chi^2}{d.o.f.} \simeq 3.1)
\end{aligned} \tag{38}$$

The theoretical uncertainties given in the results of the fits in Eq. (38) are a rough but safe estimates of the statistical errors of the fit. Actually, we have obtained a strong

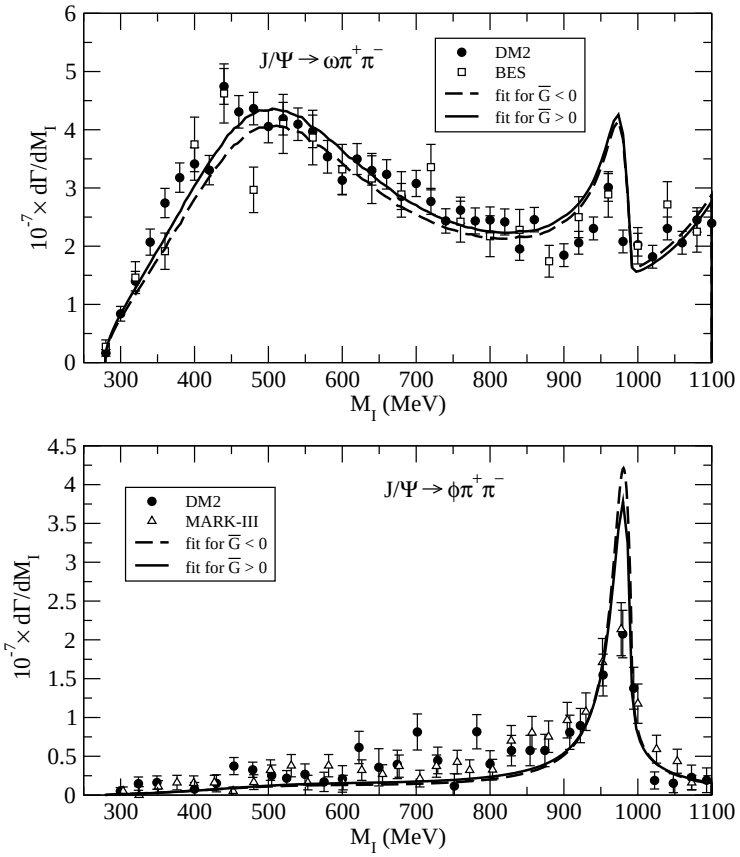

Figure 5: Results of the fits to the invariant mass distribution of the $J/\Psi \to \omega\pi^+\pi^-$ and $J/\Psi \to \phi\pi^+\pi^-$ decay channels. Solid line: result for $\overline{G} > 0$; dashed line: result for $\overline{G} < 0$.

correlation between the two parameters, (given by the off-diagonal terms of the covariance matrices), and therefore the uncertainties given in Eq. (38) are a conservative error bound extracted from the confidence ellipse of the fit. The results obtained in Eq. (38) show clearly $\lambda_\phi \neq 0$, and reasonably smaller than 1, which quantifies the OZI rule violation discussed in the present work. It is worth comparing the λ_ϕ values obtained in the present work with the one obtained in Ref. [4], $\lambda_\phi = 0.17 \pm 0.06$, which falls in the middle of our two solutions. The new mechanisms that we have introduced have definitely a relevant role in the process, but it is also rewarding that in spite of the uncertainties in the sign of $\overline{G}$, the values of λ_ϕ obtained are qualitatively similar, and also similar to the value found in Ref. [4].

In Fig. 5 we show the two results of the fits of Eq. (38) for the invariant mass distribution of the two pions in comparison with the experimental data. With the solid line we show the solution of Eq. (38) for $\overline{G} > 0$ and with dashed line the solution for $\overline{G} < 0$. The theoretical curves have to be averaged over the experimental bins since it can be specially important in the region of the $f_0(980)$ meson because of the narrowness of the distribution. We have checked that this bin average decreases the peak in the $f_0(980)$ region in the $\phi\pi\pi$ channel

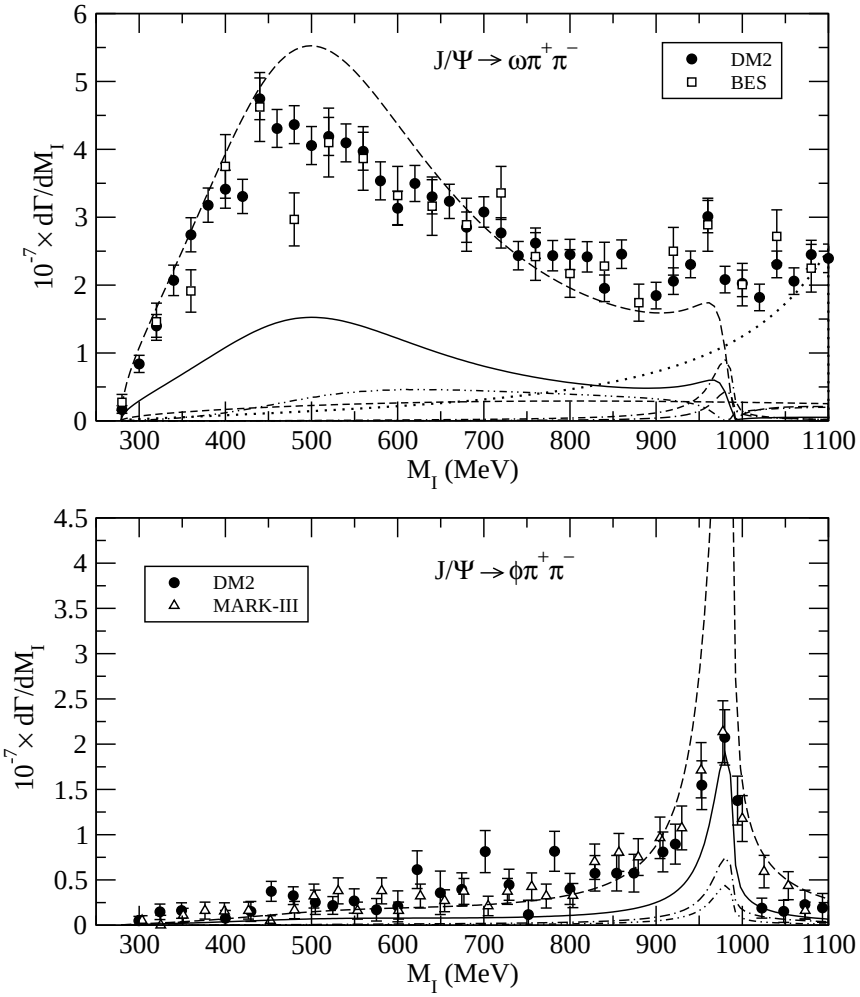

Figure 6: Different contributions to the $\pi^+\pi^-$ invariant mass distribution. The nomenclature of the different lines are explained in the text.

in around 15% and smooths a little bit the curve at these masses in the $\omega\pi\pi$ channel, but we have not plotted it for simplicity. We observe that there is a fair agreement with the experimental data for both decay channels. Specially interesting is the good agreement in the small bump appearing in the region of the $f_0(980)$ meson in the $J/\Psi \to \omega\pi^+\pi^-$ which had not been considered before in previous theoretical works. In Fig. 5 we can see that both solutions give a very similar final result, but the contributions of the various mechanisms, specially the "direct" terms, is quite different in each case as it can be seen in Fig. 6. In Fig. 6 we show the different contributions to the invariant mass distribution coming from the various mechanisms considered in our model. For the $J/\Psi \to \omega\pi^+\pi^-$ channel the lines represent: "direct" terms for $\overline{G} > 0$ (long-dashed line), "direct" terms for $\overline{G} < 0$ (solid line), sequential vector meson exchange at tree level (short-dashed line), pion loops of sequential vector meson exchange (dash double-dotted line), kaon loops of sequential vector

meson exchange (dash-dotted line), loops of sequential exchange of $K_1(1270)$ (double-dash dotted line), tail of the $f_1(1270)$ (dotted line). The intermediate b_1 meson contribution is too small to be visible in the plot and then it has not been included in the figures. For the $J/\Psi \to \phi\pi^+\pi^-$ channel the nomenclature of the lines is the same but the double-dash dotted line represents the $K_1(1400)$ exchange contribution, the sequential vector meson exchange at tree level and with pion loops are not plotted because they give a small contribution and the $f_2(1270)$ does not give contribution. The two solutions for the "direct" terms (for $\overline{G} > 0$ and $\overline{G} < 0$) look very different both in shape and in strength, indicating the important role of the $\widetilde{g}$ and λ_ϕ parameters because of the strong and non trivial interferences of the "direct" terms with the other mechanisms. In the $\omega\pi\pi$ channel, for $\overline{G} > 0$ the interference with the rest of diagrams is mainly destructive and for $\overline{G} < 0$ it is constructive. In the $\phi\pi\pi$ channel the interferences are the other way around. Specially crucial is the interference between all the mechanisms in the $f_0(980)$ region, since many diagrams contribute to it due to the final meson-meson state interaction. Therefore it is not trivial to reproduce the good strength and shape in the $f_0(980)$ region. It is important to stress again that there is no freedom in the extra mechanisms besides the "direct" terms. Therefore, their strength and shape are crucial in order to determine the free parameters of the "direct" terms when the fit with the full model to the mass distribution with absolute normalization is performed.

Special attention and discussion deserves the low mass region in the $\omega\pi\pi$ channel: the visible bump at ~ 500 MeV has been claimed in the literature to be a direct effect of the σ meson, but we will see that one has to make a very careful analysis if one wants to extract the physical σ mass and width from this reaction. In previous analyses of the DM2 data [1,8] the authors used two s-wave Breit-Wigner plus polynomial shapes ignoring their mutual interference. In the analysis of Ref. [7] using the BES data, a slightly modified BW shape was used but without considering possible interferences with other terms. We will see in the following that the correct shape of the bump at lower energies comes mainly from a subtle interference of the $t^{I=0}_{\pi\pi,\pi\pi}$ amplitudes of Fig. 1b) with the contact term of Fig. 1a). In Fig. 7 we plot the modulus squared of $G_{KK}t^{I=0}_{KK,\pi\pi}$ (dashed-dotted line), $G_{\pi\pi}t^{I=0}_{\pi\pi,\pi\pi}$ (solid line) and $1 + G_{\pi\pi}t^{I=0}_{\pi\pi,\pi\pi}$ (dashed line). In the unitary chiral models, the scalar mesons appear as poles in the second Riemann sheet of the $t_{MM,M'M'}$ scattering amplitude in the scalar-isoscalar channel [16,19]. Actually the $f_0(980)$ appears in the $987 - i14$ MeV position and the σ meson in $445 - i221$ MeV, but its physical mass, given by the distribution in the real axis, is around 600 MeV because of the large width and the complicated distribution in the complex plane of the σ meson pole [16]. Therefore the σ bump would be seen in around 600 MeV if only the term containing the $t^{I=0}_{\pi\pi,\pi\pi}$ amplitude would be present, this is, with a shape similar to the solid line in Fig. 7. When the $t^{I=0}_{\pi\pi,\pi\pi}$ term interferes with the contact term of Fig. 1a), represented by the "1" in the formulae, the shape in the σ region is strongly modified to something much more similar to the final shape of the $d\Gamma/dM_I$ curve. Therefore one can conclude that when doing an analysis of the experimental data to extract the σ mass and width one has to allow the σ meson amplitude to interfere with a polynomial containing at least the constant term. A similar narrow $\pi^+\pi^-$ distribution is found experimentally in the $J/\Psi \to p\bar{p}\pi^+\pi^-$ decay [32] and the theoretical explanation

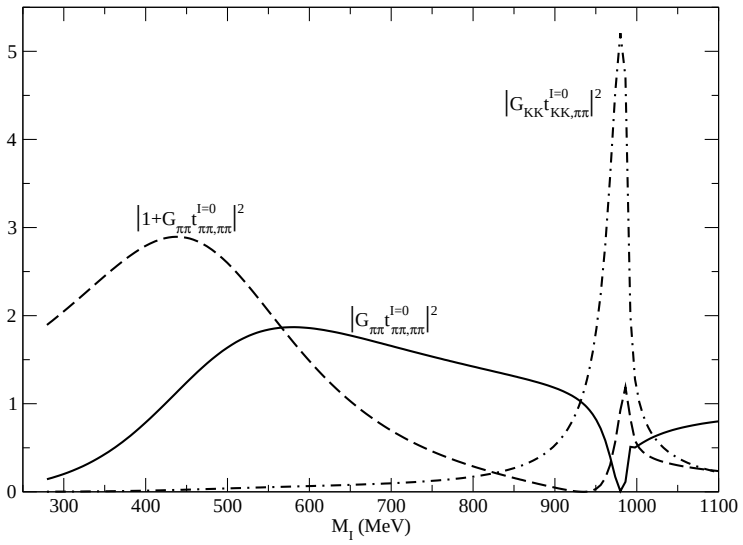

Figure 7: Modulus square of the different pieces in Eq. (18) involving the two meson loop and the meson-meson unitarized amplitude.

found in [15] was analogous to the one found here, from the interference of a tree level mechanism with a rescattering mechanism involving the $\pi\pi$ scattering matrix in the "σ" channel. This situation is different to the one found in other reactions like $\gamma\gamma \to \pi^0\pi^0$ [33], where the direct contact term is forbidden and the amplitude is dominated by the loop terms proportional to $t^{I=0}_{\pi\pi,\pi\pi}$. In this case the shape of the $\pi^0\pi^0$ distribution is very wide, resembling the solid line in Fig. 7 [33–35]. It is also interesting to present a different interpretation of this peak. Since in the σ region the $K\bar{K}$ channel is not important we can use the Bethe-Salpeter equation with only one channel, $\pi\pi$, and then we have

$$t^{I=0}_{\pi\pi,\pi\pi} = V + VG_{\pi\pi}t^{I=0}_{\pi\pi,\pi\pi} = V(1 + G_{\pi\pi}t^{I=0}_{\pi\pi,\pi\pi}). \tag{39}$$

Since in the first of Eqs. (18), neglecting the $K\bar{K}$ channel, one has the contribution $1 + G_{\pi\pi}t^{I=0}_{\pi\pi,\pi\pi}$, then one can make

$$1 + G_{\pi\pi}t^{I=0}_{\pi\pi,\pi\pi} = \frac{t^{I=0}_{\pi\pi,\pi\pi}}{V}. \tag{40}$$

Hence, the shape in the $J/\Psi \to \omega\pi^+\pi^-$ channel around $M_I = 500$ MeV is given roughly by $|t^{I=0}_{\pi\pi,\pi\pi}/V|^2$ and it happens that V ($V = -(M_I^2 - m_\pi^2/2)/f^2$) is more strongly dependent on M_I than $t^{I=0}_{\pi\pi,\pi\pi}$, it grows faster as a function of M_I and the ratio $t^{I=0}_{\pi\pi,\pi\pi}/V$ decreases faster as a function of M_I than $t^{I=0}_{\pi\pi,\pi\pi}$, producing this apparent narrower peak, which does not reflect the M_I dependence of the $t^{I=0}_{\pi\pi,\pi\pi}$ matrix but rather the M_I dependence of the kernel V. In order to see the $t^{I=0}_{\pi\pi,\pi\pi}$ amplitude one has to resort to reactions where the Born term is forbidden like in the $\gamma\gamma \to \pi^0\pi^0$ reaction.

On the other hand, by looking at Fig. 7 and Eq. (18), one can understand the different weights of the $f_0(980)$ and σ mesons in the different decay channels. From Eq. (18) one can

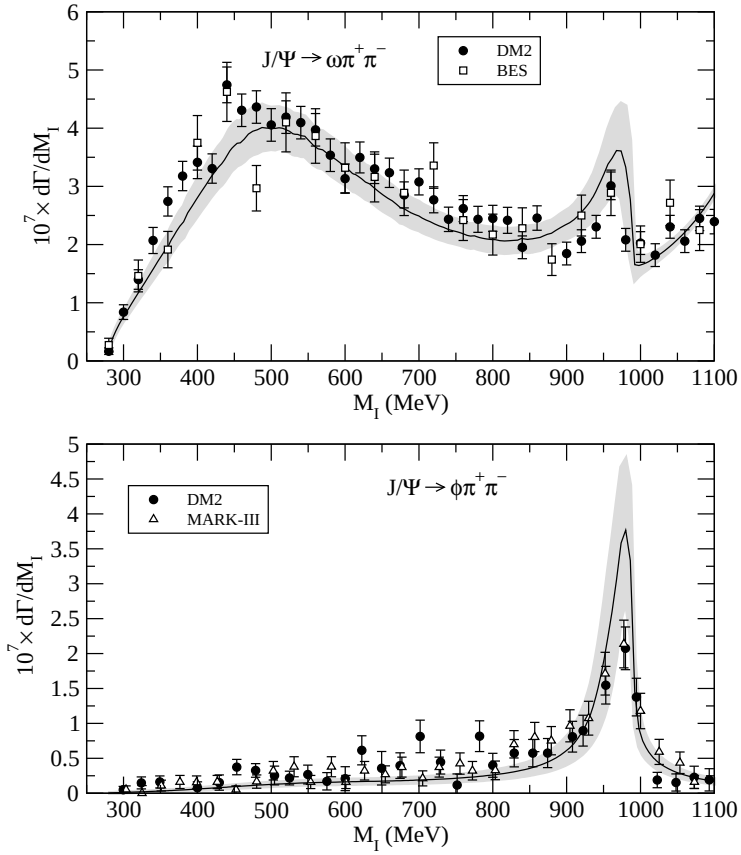

Figure 8: Final result with the theoretical error bands.

see for $J/\Psi \to \phi\pi^+\pi^-$ that the term generating the σ, $t^{I=0}_{\pi\pi,\pi\pi}$, has a coefficient $(\nu-1)$ which vanishes if the OZI rule is exact, as we pointed out before. Given the smallness of the OZI rule breaking that we have found, this term is small and hence there is practically no trace of the σ in the $J/\Psi \to \phi\pi^+\pi^-$ decay. On the other hand, there are no OZI restrictions in the coefficient of the $t^{I=0}_{KK,\pi\pi}$ amplitude, which contains the $f_0(980)$ pole, and hence the $f_0(980)$ resonance appears neatly and dominates the distribution. In the $\omega\pi^+\pi^-$ channel, the $t^{I=0}_{KK,\pi\pi}$ and $t^{I=0}_{\pi\pi,\pi\pi}$ terms are both not OZI suppressed and have comparable weight and hence both the σ and the $f_0(980)$ show up with comparable strength. This discussion is only approximate, in the sense that the final shapes and strengths are determined when added coherently to the rest of mechanisms of the model, but it describes accurately the qualitative behavior.

In order to give an idea of the uncertainties of our model, we show in Fig. 8 the final results with the theoretical error band obtaining implementing a Montecarlo gaussian sampling of the parameters used in the model within their error bounds. We only show the result for $\overline{G} < 0$, since the result for $\overline{G} > 0$ produces a very similar plot. The agreement within errors is quite fair even in the $f_0(980)$ in the $J/\Psi \to \phi\pi^+\pi^-$ channel if one would reduce by an extra $\sim 15\%$ the plot in the $f_0(980)$ region due to the experimental binning.

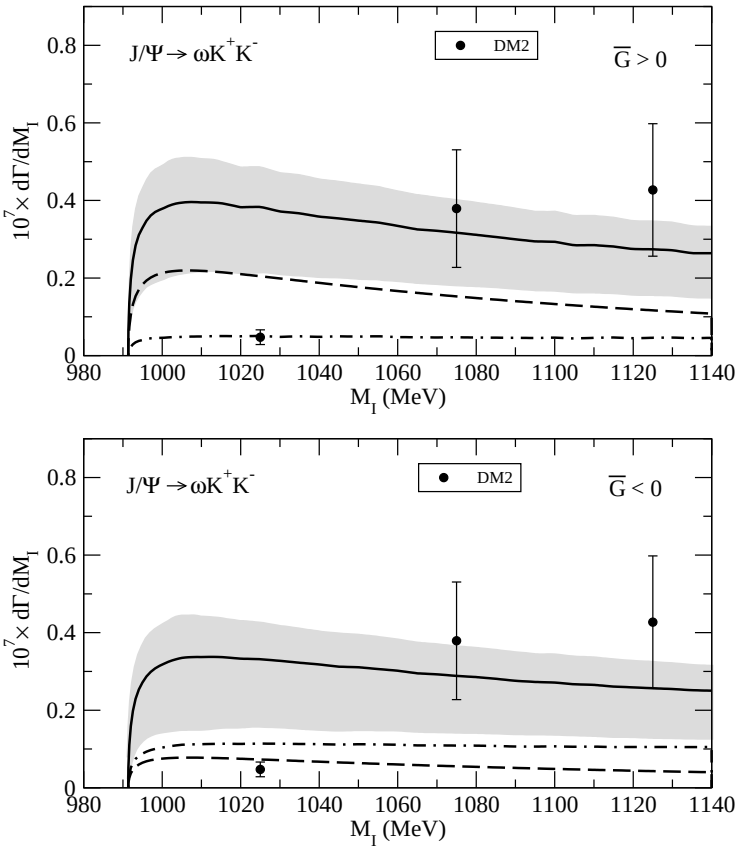

Figure 9: Results for the K^+K^- invariant mass distribution for the $J/\Psi \to \omega K^+K^-$ for the two different results of Eq. (38). Solid line: full model with the theoretical error band; dashed line: "direct" terms, dashed-dotted line: the rest of mechanisms.

With the results obtained so far, it is interesting to test the model in other decay channels having K^+K^- as final pseudoscalar pair, without introducing any extra freedom. We have thus evaluated the invariant mas distribution of the K^+K^- in $J/\Psi \to \omega K^+K^-$ and $J/\Psi \to \phi K^+K^-$ decay channels. The experimental data for the $J/\Psi \to \omega K^+K^-$ decay channel has been taken from DM2 [9] experiment. The experimental data $J/\Psi \to \phi K^+K^-$ has been taken from DM2 [9] and MARK-III [10] experiments. There are large uncertainties in the total normalization of the experimental data given the smallness of the phase space region considered. Actually one has to consider an extra $\sim 30\%$ of systematic error in the experimental data for the ωK^+K^- channel [9] not included in the data shown. We present in Figs. 9 and 10 the results for both solutions of Eq. (38) showing the contribution of the "direct" mechanisms (dashed line), all the rest of diagrams together (dashed-dotted line) and the final result with the theoretical error band (solid line). It is important to stress that nothing has been fitted in these channels, meaning that we are using the same results of Eq. (38). We see again the important role played by the interferences between the "direct" terms and the rest of diagrams in order to obtain the final shape and strength

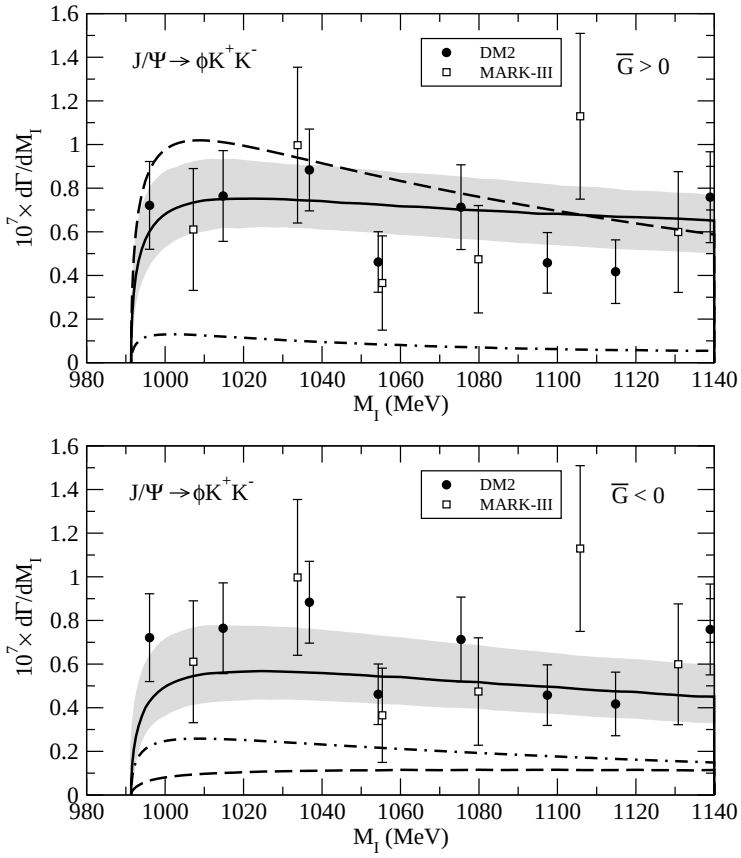

Figure 10: Results for the K^+K^- invariant mass distribution for the $J/\Psi \to \phi K^+K^-$ for the two different results of Eq. (38). Solid line: full model with the theoretical error band; dashed line: "direct" terms, dashed-dotted line: the rest of mechanisms.

of the invariant mass distributions. In the plots of both channels one can see the trend of the curve accumulating strength close to the threshold, given the proximity of the $f_0(980)$ resonance below threshold. The agreement of the results is quite fair, giving the large experimental uncertainties, also in the normalization, and the non trivial $f_0(980)$ meson effect.

It is remarkable that the strength of the direct" terms is very different in these cases. It is very large for the case $\overline{G} > 0$ and quite small for $\overline{G} < 0$, particularly in the $J/\Psi \to \phi K^+K^-$ channel, in spite of which the final results are very similar and this experiment does not help to discriminate between both solutions. The study of these K^+K^- decay processes shows however how important the "non direct" mechanisms are for these processes.

4 Conclusions

We have made a comprehensive study of the J/Ψ decay into one vector meson and two pseudoscalars, addressing mainly questions about the scalar mesons and the role played by the OZI rule. Apart from "direct" mechanisms used in previous works, we have included other mechanisms which proved relevant in similar reactions. The first and most important mechanism considered is the one containing the "direct" $J/\Psi VPP$ vertex implementing also the final state interaction of the pseudoscalar pair, following the techniques of the chiral unitary approach, which allows to extend the predictive power of ChPT up to energies $\sim$ 1.2 GeV. This chiral unitary approach implements unitarity in coupled channels and many resonances, specially the scalar mesons, are generated dynamically, showing up as poles in the meson-meson scattering amplitudes. The $J/\Psi VPP$ vertex amplitudes have been constructed using $SU(3)$ arguments to relate the different channels and also parametrizing the amplitudes in a way which clearly manifest the role of the OZI rule. We have also included in the model other mechanisms where the J/Ψ decays into a vector or axial-vector and a pseudoscalar meson and vector or axial-vector meson subsequently decays into the final vector and another pseudoscalar meson. For the J/Ψ to vector and axial-vector coupling, we have proposed a suitable phenomenological Lagrangian. We have also implemented in this mechanisms the final meson-meson state interaction which has turned out to be important in our results, since it dynamically generates the scalar mesons. These mechanisms are crucial to determine the final shape and strength of the invariant mass distribution through interferences with the "direct" terms. Given the fact that the strength of these sequential vector and axial-vector exchange mechanisms is fixed, it was important to carry a fit to the data with absolute normalization in order to obtain meaningful values for the parameters of the "direct" terms.

The only two free parameters in our model are the coupling of the direct $J/\Psi VPP$ vertex and the OZI rule violation parameter, λ_ϕ. Fitting our model to the $J/\Psi \to \omega\pi^+\pi^-$ and $J/\Psi \to \phi\pi^+\pi^-$ experimental data we obtain values of λ_ϕ clearly different from zero and reasonably smaller than one, what manifests the OZI rule violation within reasonable values.

Concerning the scalar mesons, it is important to stress first that the final shape and

strength of the bump appearing in the $\pi\pi$ invariant mass distribution in the $\omega\pi\pi$ channel at ~ 500 MeV is determined by a subtle interference between the final state interaction in the direct $J/\Psi VPP$ mechanisms and the tree level direct $J/\Psi VPP$ decay. This means that the shape and position of the bump does not directly represent the physical properties of the σ meson, since it is distorted due to interferences with other terms not related to the σ meson. Alternatively, we also showed that the relative narrowness of the peak was due to the stronger M_I dependence of the kernel V of the Bethe-Salpeter equation rather than the M_I dependence of the $t^{I=0}_{\pi\pi,\pi\pi}$ scattering amplitude. Therefore one has to be extremely careful when using the experimental data to extract the physical σ meson properties by fitting Breit-Wigner-like shapes.

On the other hand, the relative weights of the $f_0(980)$ and the σ meson are well reproduced in both the $\omega\pi\pi$ and $\phi\pi\pi$ channels in spite of their large difference in these channels. This relative weight is mainly determined by the OZI rule violation parameter and the interferences of the "direct" terms with the other mechanisms, specially in the $f_0(980)$ region. In our model, since the scalar mesons are dynamically generated through the resummed meson-meson amplitude, the relative weight between the $f_0(980)$ and the σ mesons is related to the relative weight between the $K\bar{K} \to \pi\pi$ and $\pi\pi \to \pi\pi$, in $I = 0$, scattering amplitudes. Specially remarkable is the agreement in the $f_0(980)$ region of the $\omega\pi\pi$ channel despite the smallness of the bump.

Finally, we have applied our results to the $\omega K\bar{K}$ and $\phi K\bar{K}$ decay channels, obtaining a fair agreement without introducing any extra freedom in the model. This is a nice test of the present model, both reproducing the absolute strength, and also the shape, which shows much strength close to threshold as a reflection of the proximity of the $f_0(980)$ resonance below threshold.

In conclusion, we have obtained a good description of these interesting J/Ψ decays combining phenomenological Lagrangians and the techniques of the chiral unitary approach to implement the final state rescattering of the pseudoscalar pairs, quantifying the controversial non-trivial role of the scalar mesons and the violation of the OZI rule. The fact that once more one is able to reproduce the shape and strength of the $f_0(980)$ and the σ resonances without the need to introduce them as explicit degrees of freedom provides an extra support to the idea of the nature of these resonances as dynamically generated from the interaction of the mesons.

Acknowledgments

Two of us, J.E.P. and L.R., acknowledge support from the Ministerio de Educación, Cultura y Deportes. This work is partly supported by DGICYT contract number BFM2003-00856, and the E.U. EURIDICE network contract no. HPRN-CT-2002-00311.

Appendix: Amplitudes for all the decay channels

A.1: Meson loops from direct $J/\Psi PPV$ vertex

The amplitudes for these mechanisms for all the channels are given in Eq. (18)

A.2: Sequential vector meson exchange: tree level

- $J/\Psi \to \omega\pi^+\pi^-$:

$$t = -\frac{G\overline{G}}{\sqrt{2}}\left[\frac{P^2\{a\}+\{b(P)\}}{M_\rho^2 - P^2 - iM_\rho\Gamma_\rho(P^2)} + \frac{P'^2\{a\}+\{b(P')\}}{M_\rho^2 - P'^2 - iM_\rho\Gamma_\rho(P'^2)}\right] \tag{41}$$

where $P = p_1 + q$, $P' = p_2 + q$ and

$$\{a\} = \epsilon^*\cdot\epsilon\ q^*\cdot q - \epsilon^*\cdot q\ \epsilon\cdot q^*$$
$$\{b(P)\} = -\epsilon^*\cdot\epsilon\ q^*\cdot P\ q\cdot P - \epsilon\cdot P\ \epsilon^*\cdot P\ q^*\cdot q + \epsilon^*\cdot q\ \epsilon\cdot P\ q^*\cdot P + \epsilon\cdot q^*\ \epsilon^*\cdot P\ q\cdot P$$

- $J/\Psi \to \phi\pi^+\pi^-$:

$$t = 0 \tag{42}$$

- $J/\Psi \to \omega K^+K^-$:

The diagrams are like in Fig. 2 channel but changing ρ by K^* and pions by kaons.

$$t = -\frac{G\overline{G}}{2\sqrt{2}}\left[\frac{P^2\{a\}+\{b(P)\}}{M_{K^*}^2 - P^2 - iM_{K^*}\Gamma_{K^*}(P^2)} + \frac{P'^2\{a\}+\{b(P')\}}{M_{K^*}^2 - P'^2 - iM_{K^*}\Gamma_{K^*}(P'^2)}\right] \tag{43}$$

- $J/\Psi \to \phi K^+K^-$:
The diagrams are like in the ωK^+K^- case changing ω by ϕ.

$$t = -\frac{G\overline{G}}{2}\left[\frac{P^2\{a\}+\{b(P)\}}{M_{K^*}^2 - P^2 - iM_{K^*}\Gamma_{K^*}(P^2)} + \frac{P'^2\{a\}+\{b(P')\}}{M_{K^*}^2 - P'^2 - iM_{K^*}\Gamma_{K^*}(P'^2)}\right] \tag{44}$$

A.3: Sequential axial-vector meson exchange: tree level

- $J/\Psi \to \omega\pi^+\pi^-$:

$$t = \frac{4\sqrt{2}D\overline{D}}{Mm_\omega m_b^2}\left[(\epsilon^*\cdot\epsilon\ q^*\cdot q - \epsilon^*\cdot q\ \epsilon\cdot q^*)\ +\ \frac{1}{M_b^2 - P^2 - iM_b\Gamma_b(P^2)}\cdot\right. \tag{45}$$
$$\left.\cdot\ (\epsilon^*\cdot\epsilon\ q^*\cdot P\ q\cdot P + \epsilon\cdot P\ \epsilon^*\cdot P\ q^*\cdot q - \epsilon^*\cdot q\ \epsilon\cdot P\ q^*\cdot P - \epsilon\cdot q^*\ \epsilon^*\cdot P\ q\cdot P)\right]$$

plus the crossed one, with P'.

- $J/\Psi \to \phi\pi^+\pi^-$:

$$t = 0 \tag{46}$$

- $J/\Psi \to \omega K^+K^-$:
Intermediate $K_1(1270)$:
The diagrams are like in Fig. 2 changing ρ by $K_1(1270)$ and pions by kaons.

$$t = \frac{4c\overline{D}(cD - sF)}{\sqrt{2}Mm_\omega m^2_{K_1(1270)}} \left[(\epsilon^* \cdot \epsilon \; q^* \cdot q - \epsilon^* \cdot q \; \epsilon \cdot q^*) \; + \; \frac{1}{M^2_{K_1(1270)} - P^2 - iM_{K_1(1270)}\Gamma_{K_1(1270)}(P^2)} \cdot \right.$$
$$\left. \cdot \; (\epsilon^* \cdot \epsilon \; q^* \cdot P \; q \cdot P + \epsilon \cdot P \; \epsilon^* \cdot P \; q^* \cdot q - \epsilon^* \cdot q \; \epsilon \cdot P \; q^* \cdot P - \epsilon \cdot q^* \; \epsilon^* \cdot P \; q \cdot P) \right] \tag{47}$$

plus the crossed one, with P'. $c \equiv \cos\alpha$, $s \equiv \sin\alpha$.

Intermediate $K_1(1400)$:
All the diagrams with intermediate $K_1(1270)$ also have the corresponding one with $K_1(1400)$. The amplitudes are the same but changing $m_{K_1(1270)} \to m_{K_1(1400)}$, $F \to -F$, $c \to s$ and $s \to c$. Therefore we will not explicitly give in what follows the $K_1(1400)$ case.

- $J/\Psi \to \phi K^+K^-$:

$$t = \frac{4c\overline{D}(cD - sF)}{Mm_\phi m^2_{K_1(1270)}} \left[(\epsilon^* \cdot \epsilon \; q^* \cdot q - \epsilon^* \cdot q \; \epsilon \cdot q^*) \; + \; \frac{1}{M^2_{K_1(1270)} - P^2 - iM_{K_1(1270)}\Gamma_{K_1(1270)}(P^2)} \cdot \right.$$
$$\left. \cdot \; (\epsilon^* \cdot \epsilon \; q^* \cdot P \; q \cdot P + \epsilon \cdot P \; \epsilon^* \cdot P \; q^* \cdot q - \epsilon^* \cdot q \; \epsilon \cdot P \; q^* \cdot P - \epsilon \cdot q^* \; \epsilon^* \cdot P \; q \cdot P) \right] \tag{48}$$

A.4: Loops of sequential vector meson exchange

- $J/\Psi \to \omega\pi^+\pi^-$

Pion loops:

$$t^{\mu\nu} = \frac{G\overline{G}}{\sqrt{2}} \, \bar{t}'^{\mu\nu} \, 2t^{I=0}_{\pi\pi,\pi\pi} \tag{49}$$

$\bar{t}'^{\mu\nu}$ is given in Eq. (32), but using proper masses and widths in the evaluation.

Kaon loops:

$$t^{\mu\nu} = \frac{G\overline{G}}{2\sqrt{2}}\,\bar{t}'^{\mu\nu}\,\frac{4}{\sqrt{3}}t^{I=0}_{KK,\pi\pi} \tag{50}$$

- $J/\Psi \to \phi\pi^+\pi^-$:

Pion loops:

$$t^{\mu\nu} = 0 \tag{51}$$

Kaon loops:
The diagrams are like in Fig. 4 changing ω by ϕ.

$$t^{\mu\nu} = \frac{G\overline{G}}{2}\,\bar{t}'^{\mu\nu}\,\frac{4}{\sqrt{3}}t^{I=0}_{KK,\pi\pi} \tag{52}$$

- $J/\Psi \to \omega K^+K^-$:

Pion loops:
The diagrams are like in Fig. 3 changing the final $\pi^+\pi^-$ by K^+K^-.

$$t^{\mu\nu} = \frac{G\overline{G}}{\sqrt{2}}\,\bar{t}'^{\mu\nu}\,\sqrt{\frac{3}{2}}t^{I=0}_{\pi\pi,KK} \tag{53}$$

Kaon loops:

$$t^{\mu\nu} = \frac{G\overline{G}}{2\sqrt{2}}\,\bar{t}'^{\mu\nu}\,2t^{I=0}_{KK,KK} \tag{54}$$

- $J/\Psi \to \phi K^+K^-$:

Pion loops:

$$t^{\mu\nu} = 0 \tag{55}$$

Kaon loops:
The diagrams are like in the ωK^+K^- case changing ω by ϕ.

$$t^{\mu\nu} = \frac{G\overline{G}}{2}\,\bar{t}'^{\mu\nu}\,2t^{I=0}_{KK,KK} \tag{56}$$

A.5: Loops of sequential axial-vector meson exchange

- $J/\Psi \to \omega\pi^+\pi^-$:

Pion loops:

$$t^{\mu\nu} = \frac{4\sqrt{2}D\overline{D}}{Mm_\omega m_b^2}\left[(q^*\cdot qg^{\mu\nu} - q^\mu q^{*\nu})G_{\pi\pi} - \tilde{t}'^{\mu\nu}\right] 2t^{I=0}_{\pi\pi,\pi\pi} \tag{57}$$

See subsection 2.3 for definition of $\tilde{t}'^{\mu\nu}$ and the momenta.

Kaon loops:

$$t^{\mu\nu} = \frac{4}{Mm_\omega m^2_{K_1(1270)}} c\overline{D}\frac{1}{\sqrt{2}}(cD - sF)\left[(q^*\cdot qg^{\mu\nu} - q^\mu q^{*\nu})G_{KK} - \tilde{t}'^{\mu\nu}\right]\frac{4}{\sqrt{3}}t^{I=0}_{KK,\pi\pi} \tag{58}$$

- $J/\Psi \to \phi\pi^+\pi^-$

Pion loops:

$$t^{\mu\nu} = 0 \tag{59}$$

Kaon loops:

Intermediate $K_1(1270)$ meson:
The diagrams are like in Fig. 4 changing K^* by $K_1(1270)$ and ω by ϕ.

$$t^{\mu\nu} = \frac{4}{Mm_\phi m^2_{K_1(1270)}} c\overline{D}(cD + sF)\left[(q^*\cdot qg^{\mu\nu} - q^\mu\cdot q^{*\nu})G_{KK} - \tilde{t}'^{\mu\nu}\right]\frac{4}{\sqrt{3}}t^{I=0}_{KK,\pi\pi} \tag{60}$$

- $J/\Psi \to \omega K^+K^-$:

Pion loops:
The diagrams are like in Fig. 3 changing ρ by b_1 and the final $\pi^+\pi^-$ by K^+K^-.

$$t^{\mu\nu} = \frac{4\sqrt{2}D\overline{D}}{Mm_\omega m_b^2}\left[(q^*\cdot qg^{\mu\nu} - q^\mu q^{*\nu})G_{\pi\pi} - \tilde{t}'^{\mu\nu}\right]\sqrt{3}t^{I=0}_{\pi\pi,KK} \tag{61}$$

Kaon loops:
The diagrams are like in Fig. 4 changing K^* by $K_1(1270)$ and the final $\pi^+\pi^-$ by K^+K^-.

$$t^{\mu\nu} = \frac{4}{Mm_\omega m^2_{K_1(1270)}} c\overline{D}\frac{1}{\sqrt{2}}(cD - sF)\left[(q^*\cdot qg^{\mu\nu} - q^\mu q^{*\nu})G_{KK} - \tilde{t}'^{\mu\nu}\right] 2t^{I=0}_{KK,KK} \tag{62}$$

- $J/\Psi \to \phi K^+K^-$:

Pion loops:

$$t^{\mu\nu} = 0 \tag{63}$$

Kaon loops:
The diagrams are like in the ωK^+K^- case changing ω by ϕ.

$$t^{\mu\nu} = \frac{4}{Mm_\phi m^2_{K_1(1270)}} c\overline{D}(cD + sF)\left[(q^* \cdot q g^{\mu\nu} - q^\mu \cdot q^{*\nu})G_{KK} - \tilde{t}'^{\mu\nu}\right] 2t^{I=0}_{KK,KK} \tag{64}$$

References

[1] K. Takamatsu, M. Ishida, S. Ishida, T. Ishida and T. Tsuru, arXiv:hep-ph/9712232.

[2] D. Morgan and M. R. Pennington, Phys. Rev. D **48** (1993) 5422.

[3] M. Uehara, Prog. Theor. Phys. **109** (2003) 265 [arXiv:hep-ph/0211029].

[4] U. G. Meissner and J. A. Oller, Nucl. Phys. A **679** (2001) 671 [arXiv:hep-ph/0005253].

[5] G. Janssen, B. C. Pearce, K. Holinde and J. Speth, Phys. Rev. D **52** (1995) 2690 [arXiv:nucl-th/9411021].

[6] R. Escribano, A. Gallegos, J. L. Lucio M, G. Moreno and J. Pestieau, Eur. Phys. J. C **28** (2003) 107 [arXiv:hep-ph/0204338].

[7] N. Wu, arXiv:hep-ex/0104050.

[8] J. E. Augustin *et al.* [DM2 Collaboration], Nucl. Phys. B **320** (1989) 1.

[9] A. Falvard *et al.* [DM2 Collaboration], Phys. Rev. D **38** (1988) 2706.

[10] W. S. Lockman [MARK-III Collaboration], SLAC-PUB-5139 *Presented at 3rd Int. Conf. on Hadron Spectroscopy, Ajaccio, France, Sep 23-27, 1989*

[11] Proc. of the Workshop on the "Possible existence of the σ meson and its implication in hadron physics", Kyoto June, 2000, Ed. S. Ishida et al., web page http://amaterasu.kek.jp/YITPws/.

[12] N. N. Achasov and V. N. Ivanchenko, Nucl. Phys. B **315** (1989) 465.

[13] M. Boglione and M. R. Pennington, Eur. Phys. J. C **30** (2003) 503 [arXiv:hep-ph/0303200].

[14] J. E. Palomar, L. Roca, E. Oset and M. J. Vicente Vacas, Nucl. Phys. A **729** (2003) 743 [arXiv:hep-ph/0306249].

[15] C. b . Li, E. Oset and M. J. Vicente Vacas, Phys. Rev. C **69** (2004) 015201 [arXiv:nucl-th/0305041].

[16] J. A. Oller, E. Oset and J. R. Pelaez, Phys. Rev. D **59** (1999) 074001 [Erratum-ibid. D **60** (1999) 099906] [arXiv:hep-ph/9804209].

[17] J. A. Oller and E. Oset, Phys. Rev. D **60** (1999) 074023 [arXiv:hep-ph/9809337].

[18] J. A. Oller, E. Oset and A. Ramos, Prog. Part. Nucl. Phys. **45** (2000) 157 [arXiv:hep-ph/0002193].

[19] J. A. Oller and E. Oset, Nucl. Phys. A **620** (1997) 438 [Erratum-ibid. A **652** (1999) 407] [arXiv:hep-ph/9702314].

[20] S. Descotes-Genon, L. Girlanda and J. Stern, JHEP **0001** (2000) 041 [arXiv:hep-ph/9910537].

[21] N. Isgur and H. B. Thacker, Phys. Rev. D **64** (2001) 094507 [arXiv:hep-lat/0005006].

[22] A. Bramon, R. Escribano, J. L. Lucio Martinez and M. Napsuciale, Phys. Lett. B **517** (2001) 345 [arXiv:hep-ph/0105179].

[23] A. Bramon, A. Grau and G. Pancheri, Phys. Lett. B **289** (1992) 97.

[24] L. Roca, J. E. Palomar and E. Oset, arXiv:hep-ph/0306188.

[25] J. Gasser and H. Leutwyler, Nucl. Phys. B **250** (1985) 465.

[26] J. E. Palomar, S. Hirenzaki and E. Oset, Nucl. Phys. A **707** (2002) 161 [arXiv:hep-ph/0111308].

[27] N. N. Achasov and A. V. Kiselev, Phys. Rev. D **68** (2003) 014006 [arXiv:hep-ph/0212153].

[28] A. Bramon, R. Escribano, J. L. Lucio M, M. Napsuciale and G. Pancheri, Eur. Phys. J. C **26** (2002) 253 [arXiv:hep-ph/0204339].

[29] K. Hagiwara *et al.* [Particle Data Group Collaboration], Phys. Rev. D **66** (2002) 010001.

[30] M. Suzuki, Phys. Rev. D **47** (1993) 1252.

[31] G. Ecker, J. Gasser, A. Pich and E. de Rafael, Nucl. Phys. B **321** (1989) 311.

[32] M. W. Eaton *et al.*, Phys. Rev. D **29** (1984) 804.

[33] J. A. Oller and E. Oset, Nucl. Phys. A **629** (1998) 739 [arXiv:hep-ph/9706487].

[34] H. Marsiske *et al.* [Crystal Ball Collaboration], Phys. Rev. D **41** (1990) 3324.

[35] T. Oest *et al.* [JADE Collaboration], Z. Phys. C **47** (1990) 343.